

# Square-wave oscillations in semiconductor ring lasers with delayed optical feedback

Lilia Mashal\*, Guy Van der Sande, Lendert Gelens, Jan Danckaert, and Guy Verschaffelt

Applied Physics Research Group (APHY), Vrije Universiteit Brussel, Pleinlaan 2,  
B-1050 Brussel, Belgium

[\\*lmashal@vub.ac.be](mailto:lmashal@vub.ac.be)

**Abstract:** We analyze experimentally and theoretically the effects of delayed optical cross-feedback in semiconductor ring lasers. We show that under appropriate conditions, feeding of only one directional mode back into the counter-propagating mode leads to square-wave oscillations. In this regime, the laser switches regularly between the two counter-propagating modes with a period close to twice the roundtrip time in the external feedback loop. We find that these oscillations are robust and appear for a wide range of parameters as long as a small asymmetry in the linear coupling between both modes is present. We show that by increasing the feedback strength or the injection current, the square-wave oscillations gradually disappear. Due to noise, mode-hopping between stable lasing in one directional mode and square wave oscillations is observed in this transition region.

© 2012 Optical Society of America

**OCIS codes:** (140.3560) Lasers, ring; (140.5960) Semiconductor lasers; Instabilities and chaos; (140.1540).

---

## References and links

1. T. Erneux and P. Glorieux, *Laser Dynamics* (Cambridge University Press, Cambridge, UK, 2010).
2. T. Erneux, *Applied Delay Differential Equations* (Springer, New York, 2009).
3. A. Argyris, D. Syvridis, L. Larger, V. Annovazzi-Lodi, P. Colet, I. Fischer, J. García-Ojalvo, C. R. Mirasso, L. Pesquera, and K. A. Shore, "Chaos-based communications at high bit rates using commercial fibre-optic links," *Nature* **438**, 343–346 (2005).
4. L. Appeltant, M. C. Soriano, G. Van der Sande, J. Danckaert, S. Massar, J. Dambre, B. Schrauwen, C. R. Mirasso, and I. Fischer, "Information processing using a single dynamical node as complex system," *Nat. Commun.* **2**, 468 (2011).
5. A. Gavrielides, T. Erneux, D. Sukow, G. Burner, T. McLachlan, J. Miller, and J. Amonette, "Square-wave self-modulation in diode lasers with polarization-rotated optical feedback," *Opt. Lett.* **13**, 2006–2008 (2006).
6. E. Viktorov, A. M. Yacomotti, and P. Mandel, "Semiconductor lasers coupled face-to-face," *J. Opt. B: Quantum Semiclass. Opt.* **6**, L9–L12 (2004).
7. J. Mulet, M. Giudici, J. Javaloyes, and S. Balle, "Square-wave switching by crossed-polarization gain modulation in vertical-cavity semiconductor lasers," *Phys. Rev. A* **76**, 043801 (2007).
8. A. Gavrielides, D. Sukow, G. Burner, T. McLachlan, J. Miller, and J. Amonette, "Simple and complex square waves in an edge-emitting diode laser with polarization-rotated optical feedback," *Phys. Rev. E* **81**, 056209 (2010).
9. D. Sukow, A. Gavrielides, T. Erneux, B. Mooneyham, K. Lee, J. McKay, and J. Davis, "Asymmetric square waves in mutually coupled semiconductor lasers with orthogonal optical injection," *Phys. Rev. E* **81**, 025206 (2010).

10. C. Masoller, D. Sukow, A. Gavrielides, and M. Sciamanna, "Bifurcation to square-wave switching in orthogonally delay-coupled semiconductor lasers: Theory and experiment," *Phys. Rev. A* **84**, 023838 (2011).
11. M. Sciamanna, M. Virte, C. Masoller, and A. Gavrielides, "Hopf bifurcation to square-wave switching in mutually coupled semiconductor lasers," to be published in *Phys. Rev. E* (2012).
12. T. Heil, A. Uchida, P. Davis, and T. Aida, "TE-TM dynamics in a semiconductor laser subject to polarization-rotated optical feedback," *Phys. Rev. A* **68**, 033811 (2003).
13. M. T. Hill, H. Dorren, T. de Vries, X. Leijtens, J. den Besten, B. Smalbrugge, Y. Oei, H. Binsma, G. Khoe, and M. Smit, "A fast low-power optical memory based on coupled micro-ring lasers," *Nature* **432**, 206–209 (2004).
14. V. R. Almeida, C. Barrios, R. Panepucci, M. Lipson, M. Foster, D. Ouzounov, and A. Gaeta, "All-optical switching on a silicon chip," *Opt. Lett.* **29**, 2867–2869 (2004).
15. L. Gelens, G. Van der Sande, S. Beri, and J. Danckaert, "Phase-space approach to directional switching in semiconductor ring lasers," *Phys. Rev. E* **79**, 016213 (2009).
16. L. Gelens, S. Beri, G. Van der Sande, G. Mezosi, M. Sorel, J. Danckaert, and G. Verschaffelt, "Exploring multistability in semiconductor ring lasers: Theory and experiment," *Phys. Rev. Lett.* **102**, 193904 (2009).
17. L. Gelens, L. Mashal, S. Beri, W. Coomans, G. Van der Sande, J. Danckaert, and G. Verschaffelt, "Excitability in semiconductor microring lasers: Experimental and theoretical pulse characterization," *Phys. Rev. A* **82**, 063841 (2010).
18. S. Beri, L. Gelens, M. Mestre, G. Van der Sande, G. Verschaffelt, A. Sciré, G. Mezosi, M. S. M, and J. Danckaert, "Topological insight into the non-Arrhenius mode hopping of semiconductor ring lasers," *Phys. Rev. Lett.* **101**, 093903 (2008).
19. M. Sorel, G. Giuliani, A. Sciré, R. Miglierina, S. Donati, and P. Laybourn, "Operating regimes of GaAs-AlGaAs semiconductor ring lasers: experiment and mode," *IEEE J. Quantum Electron.* **39**, 1187–1195 (2003).
20. G. Van der Sande, L. Gelens, P. Tassin, A. Sciré, and J. Danckaert, "Two-dimensional phase-space analysis and bifurcation study of the dynamical behavior of a semiconductor ring laser," *J. Phys. B* **41**, 095402 (2008).
21. M. Sorel, P. Laybourn, A. Sciré, S. Balle, G. Giuliani, R. Miglierina, and S. Donati, "Alternate oscillations in semiconductor ring lasers," *Opt. Lett.* **27**, 1992–1994 (2002).
22. W. Coomans, S. Beri, G. Van der Sande, L. Gelens, and J. Danckaert, "Optical injection in semiconductor ring lasers," *Phys. Rev. A* **81**, 033802 (2010).
23. L. Gelens, S. Beri, L. Mashal, G. Van der Sande, J. Danckaert, and G. Verschaffelt, "Multistable and excitable behavior in semiconductor ring lasers with broken Z2-symmetry," *Eur. Phys. J. D* **58**, 197–207 (2010).
24. M. S. Torre, A. Gavrielides, and C. Masoller, "Numerical characterization of transient polarization square-wave switching in two orthogonally coupled VCSELs," *Opt. Express* **19**, 20269–20278 (2011).
25. M. Yousefi, D. Lenstra, and G. Vemuri, "Carrier inversion noise has important influence on the dynamics of a semiconductor laser," *IEEE J. Sel. Top. Quantum Electron.* **10**, 955–960 (2004).
26. M. C. Soriano, T. Berkvens, G. Van der Sande, G. Verschaffelt, J. Danckaert and I. Fischer, "Interplay of Current Noise and Delayed Optical Feedback on the Dynamics of Semiconductor Lasers," *IEEE J. Quantum Electron.* **47**, 368–374 (2011).

## 1. Introduction

Delayed optical feedback in semiconductor laser systems has been shown to exhibit a wealth of dynamical behavior [1, 2]. It can generate an optical chaotic signal useful for e.g. chaos encryption techniques [3] and, recently it has been shown that the complex transient behavior of delayed feedback systems can even process information [4]. One particular example of a dynamical regime that can arise through time-delayed optical feedback is square-wave switching. The generation of such square-wave oscillations has received a lot of interest in the past years [5–11], both out of fundamental interest and because applications involving the production of high-frequency optical pulses have been suggested [12].

Square-wave modulation of the power emitted in each of the polarization orientations has been demonstrated in edge-emitting lasers (EELs) by using crossed-polarization re-injection (XPR) [5]. Considering such an edge-emitting, Fabry-Perot diode laser, the optical feedback from an external cavity couples asymmetrically from the natural horizontal TE polarization mode to the non-lasing, orthogonal TM mode. The main prerequisite for obtaining square-wave oscillations with a period close to twice the delay introduced by the external feedback path is that the differential losses in the TM mode are small. In this configuration, the square-wave self-modulation always has a duty cycle of about 50%. It has been shown, however, that by using two EELs coupled through polarization-rotated feedback asymmetric duty cycles can be ob-

tained as well, keeping the total period close to the roundtrip time of the feedback loop [9, 10]. A lot of attention has also been paid to studying square-wave modulation in vertical-cavity surface-emitting lasers (VCSELs) [6, 7]. In VCSELs, the losses in the orthogonal mode are typically much lower than in edge-emitting lasers. Square-waves have been observed for XPR levels above a critical value, with a period related to twice the re-injection delay as well. If the level of XPR becomes too strong, however, a degradation of the square waves has been observed and finally they disappear completely [7].

In this work, we report on the experimental and theoretical observation of square wave oscillations in semiconductor ring lasers (SRLs). SRLs are semiconductor lasers where the laser cavity consists of a ring-shaped waveguide. As a result, SRLs generate light in two opposite directions referred to as the clockwise (CW) and the counterclockwise (CCW) mode. They have been shown to be promising sources in photonic integrated circuits [13]. In particular, their possibility of bistable directional operation paved the way to encoding digital information in the direction of emission of SRLs [13, 14]. SRLs have been shown to have interesting dynamical properties due to their  $Z_2$  symmetry. The particular phase-space structure of these two-mode lasers has been used to explain alternative switching mechanisms [15], multi-stable regions of operation [16], excitability [17] and non-Arrhenius mode hopping [18].

The square-wave oscillations that we report on in this paper differ in origin from previous observations in EELs [5] and VCSELs [7] in several ways. For EELs and VCSELs, the underlying origin of the square wave behavior is attributed to a gain difference between the two modes. Without XPR, the mode with the highest gain is lasing, while the other mode has insufficient gain and remains off. Sufficiently strong delayed XPR, from the high gain mode into the low gain mode, overcomes the gain anisotropy and pushes the low gain mode above the lasing threshold, while turning off the high gain mode. This essentially kills the XPR, which will switch the laser back to the high gain mode after one delay, thus starting a new square wave cycle. While SRLs are -like VCSELs- two-mode lasers, no gain anisotropy is present between both counter-propagating modes in the SRL. Even more, because the SRL modes are linearly coupled through a physical process referred to as backscattering, they are always phase locked and both modes are always on. It is the interplay between this linear coupling and gain saturation processes that defines the mode partitioning. We show here that a certain asymmetry in linear coupling between both counter-propagating modes and the cross-saturation effects are needed in order to induce square waveforms in SRLs. Also, contrary to VCSELs, solitary SRLs show a large variety of dynamics (alternate oscillations [19], multistability [16] and excitability [17]), which will interact with the formation of square waves.

Although the square waves are stable without noise, we find that the noise strength can change the regularity of the square waves as for increasing feedback strengths or injection currents, noise-induced mode-hopping occurs between the square wave attractor and stable unidirectional CW or CCW operation. The time-delayed coupling of one directional mode back into the counter-propagating mode leads to square-wave oscillations when the feedback strength exceeds a critical value. Similar as in EELs and VCSELs, the oscillations have a duty cycle of about 50% and a period close to twice the roundtrip time in the external feedback or cross-injection loop. Finally, our numerical analysis shows that the square wave switching are accompanied by oscillations which are much slower than the relaxation oscillation timescale.

The paper is organized as follows. In Sec. 2 we describe the experimental setup and the effect of the pump current and feedback strength on the presence and properties of the square waveforms. Sec. 3 details the theoretical model and discusses the numerical results obtained. A summary and discussion are provided in Sec. 4.

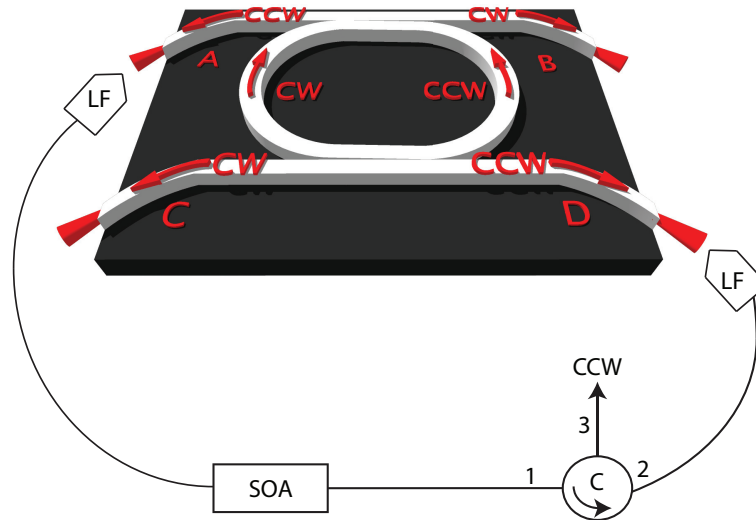


Fig. 1. A schematic view of the semiconductor ring laser and a sketch of the experimental setup. LF is the lensed fiber, SOA the semiconductor optical amplifier and C the circulator.

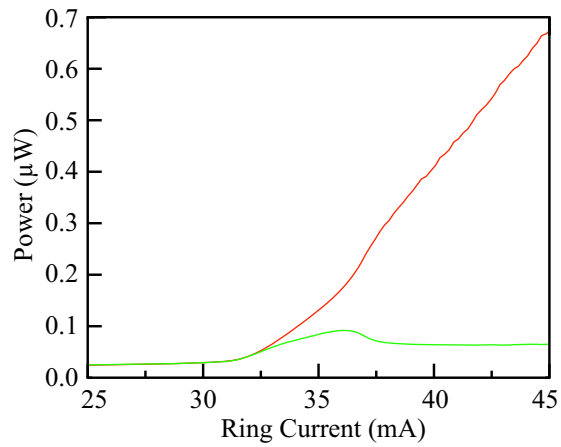


Fig. 2. SRL's optical output power in CW (green) and CCW (red) directions. Remark that the output power is fairly low, because no current is sent through the output waveguides.

## 2. Experimental results

The experiments are performed on an InP-based multi-quantum-well semiconductor ring laser (SRL). A schematic representation of such SRL is shown in Fig. 1. The geometry of the ring cavity supports two directional modes: clockwise (CW) and counterclockwise (CCW). The circumference of the SRL cavity is 1.87 mm, leading to a (experimentally measured) longitudinal mode spacing of 53.6 GHz at a center wavelength of 1.56  $\mu\text{m}$ . Directional couplers allow to couple out part of the light from the ring in the output waveguides. As shown in Fig. 1, there are four ports (A, B, C, and D) at the facets of the chip that serve as SRL inputs or outputs. Lensed optical fibers can be aligned to these ports. The device is mounted on a copper chuck and thermally controlled by a Peltier element with an accuracy of 0.01°C. In Fig. 2 we plot the optical power measured in the CW and CCW directions as a function of the SRL pumping current  $I_r$ . The SRL has a threshold current of 32 mA. Above and close to the threshold, the SRL resides in the bidirectional regime where it emits both directional modes. The CCW mode increases more strongly than the CW mode with increasing injection current. Above 37 mA, the CW mode's power drops and the SRL enters the uni-directional regime where one of the directional modes is much stronger than the other.

The feedback loop is organized using lensed fibers connected to ports A and D. The roundtrip time of the external cavity is given by  $\tau = nL/c$ , where  $L$  is the length of the external cavity,  $c$  is the speed of light and  $n$  is the refractive index of the fiber. Here  $L$  is 9.57m, leading to  $\tau \approx 47.9\text{ns}$ . A semiconductor optical amplifier (SOA) is placed in the feedback loop to control the feedback strength by changing the current in the SOA. In all of the experiments, the saturation power of the SOA (model Thorlabs SOA1117S) is larger than the input signal from the SRL that is amplified, such that the SOA is always operated in its linear gain regime. The SOA gain depends on its pump current. For a SOA current of 0 mA, the SOA is strongly absorbing. For SOA currents between 200 mA and 600 mA, the SOA gain increases approximately linearly from 7.5 dB to 20 dB. The SOA will also generate amplified spontaneous emission (ASE) noise that is injected only in the CW direction. The ASE power is 34  $\mu\text{W}$  at 200 mA and increases to 1.3 mW at a SOA current of 600 mA. This is much higher than the power emitted from the SRL, but this ASE power is emitted at all wavelengths ranging from 1520nm to 1580nm. Therefore, only a small amount of the ASE power is injected in the SRL's lasing mode, which we neglect in our analysis. The SOA is connected to port 1 of a circulator via an optical fiber. The circulator transmits light from port 1 to port 2, which in its turn is connected to port D of the SRL chip via a lensed optical fiber. Hence, the CCW directional mode of the SRL from port A of the chip is re-injected in the CW direction through port D (i.e. cross-feedback). On the contrary, the CCW mode coupled out from port D, is coupled out of the feedback loop by the circulator and is used for characterization purposes. We note that in this setup, the CCW mode is injected in the CW mode but not vice versa (asymmetric cross-feedback). Light from port 3 of the circulator is detected by a fast photodiode connected to an oscilloscope. In order to avoid optical feedback from the facets of the chip, the output waveguides are tilted by 10° with respect to the chip facets. Therefore, the fibers are angled at 32° with respect to the facet's normal. As the output waveguides at Ports A-D are fabricated from the same active material as the ring waveguide, they will be highly absorbing. Therefore, an independent bias current  $I_{WG}$  is provided to the output waveguide of port D in order to increase the amount of light coupled to the feedback section.

First we fix the injection current on the SOA ( $I_{SOA} = 0.3\text{ A}$ ) and we vary the pumping current  $I_r$  on the SRL. In Fig. 3 we show typical time traces of the CCW mode of the SRL for three different values of the pumping current  $I_r$ . Without feedback (i.e. for  $I_{SOA} = 0\text{mA}$ ), the SRL operates in the unidirectional regime for pumping currents  $I_r$  larger than 40mA (not shown). In accordance with previous work, we refer to unidirectional operation if one of the counter-

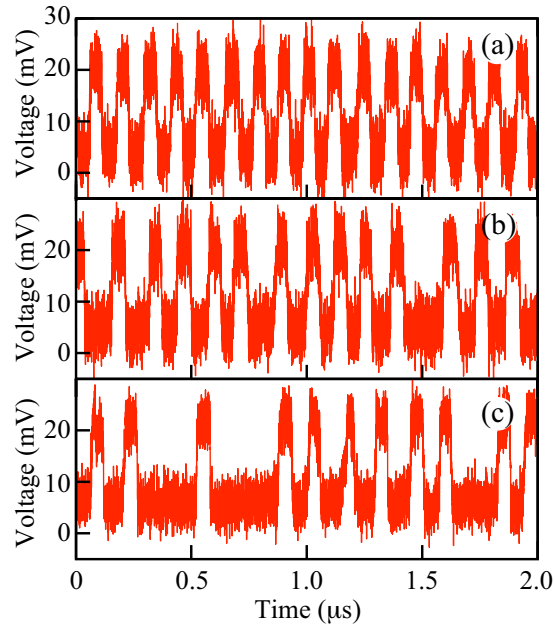


Fig. 3. Time traces of the CCW mode. Parameters are (a)  $I_r = 42\text{mA}$ ,  $I_{SOA} = 300\text{mA}$  and  $I_{WG} = 10\text{mA}$ , (b)  $I_r = 43\text{mA}$ ,  $I_{SOA} = 300\text{mA}$  and  $I_{WG} = 10\text{mA}$  and (c)  $I_r = 44\text{mA}$ ,  $I_{SOA} = 300\text{mA}$  and  $I_{WG} = 10\text{mA}$ . The temperature is stabilized at  $23^\circ\text{C}$ .

propagating modes has much more intensity than the other mode [19, 20]. Measurements of the optical spectrum (also not shown) confirm that the SRL lases in a single longitudinal mode under all experimental conditions reported in this paper. If we set the laser current at  $42\text{mA}$  and turn on the feedback by changing the SOA current to  $300\text{mA}$  (see Fig. 3a), square waves appear with a period of approximately  $122\text{ns}$ . This period is close to twice the round trip time in the external cavity. In Figs. 3(b) and 3(c) we increase the laser current while keeping the SOA current fixed. At a laser current of  $43\text{mA}$  [see Fig. 3(b)], the square waves become slightly irregular. This irregularity gets more pronounced as we further increase the pump current as can be seen in Fig. 3(c) at an injection current of  $44\text{mA}$ . In Fig. 3(c), the SRL sometimes resides in the CW mode such that some of the square wave cycles are missed. Nevertheless, when a square wave cycle is performed, this cycle still has the same shape and period as in Fig. 3(a).

A similar scenario is found when the pumping current  $I_r$  on the SRL is fixed and the feedback strength is varied (by changing the current in the SOA) as can be seen from the time traces presented in Fig. 4. Without feedback [see Fig. 4(a)], the SRL emits in the CCW direction. For a SOA current in the range of  $150\text{mA}$ - $250\text{mA}$ , we observe [see Fig. 4(b)] regular square wave intensity oscillations in the CCW mode's output power. When we further increase the feedback strength, we first see bursts of square waves surrounded by regions of CW emission [see Fig. 4(c)]. For even higher feedback strengths [see Fig. 4(d)], the SRL mostly resides in the CW mode with some irregularly distributed pulses to the CCW mode.

### 3. Numerical results

In order to interpret our experimental results we assume that the SRL operates in a single transverse and longitudinal mode and use a model formulated mathematically in terms of two rate



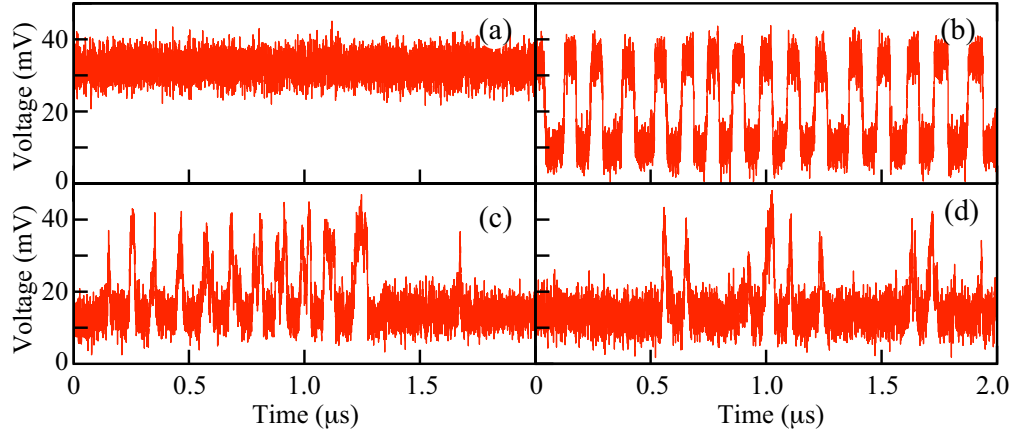


Fig. 4. Time traces of the CCW mode. Parameters are  $I_r = 43$  mA,  $I_{WG} = 10$  mA, (a)  $I_{SOA} = 0$  mA, (b)  $I_{SOA} = 200$  mA, (c)  $I_{SOA} = 400$  mA, and (d)  $I_{SOA} = 500$  mA.

equations for the slowly varying amplitudes  $E_{cw,ccw}$  of the two counter-propagating modes and one rate equation for the carrier number  $N$ . This two-mode model for a solitary SRL was initially proposed in [19, 21] and was used successfully to study optical injection in SRLs [22], non-Arrhenius mode hopping [18], excitability [17] and multistability [16]. The model we consider is given by

$$\dot{E}_{ccw} = \kappa(1 + i\alpha)(G_{ccw}N - 1)E_{ccw} - k(1 + \delta k)e^{i\phi_k}E_{cw} + \tilde{F}_{ccw}, \quad (1)$$

$$\dot{E}_{cw} = \kappa(1 + i\alpha)(G_{cw}N - 1)E_{cw} - k(1 - \delta k)e^{i\phi_k}E_{ccw} - \eta e^{i\theta}E_{ccw}(t - \tau) + \tilde{F}_{cw}, \quad (2)$$

$$\dot{N} = \gamma(\mu - N - NG_{cw}|E_{cw}|^2 - NG_{ccw}|E_{ccw}|^2). \quad (3)$$

In order to account for the delayed optical injection from the CCW mode in the CW mode, we have included a delayed feedback term of Lang-Kobayashi type in Eq. (2) with feedback strength  $\eta$ , feedback phase  $\theta$  and delay time  $\tau=50$  ns. Eqs. (1)-(3) contain two necessary ingredients to correctly describe the mode competition in SRLs [20]: backscattering and gain saturation.

Backscattering of the counterpropagating modes can be caused by index variations within the ring cavity, at the interface between the circular cavity and the straight coupling waveguide and at the end facets of the output waveguides. These reflections result in a linear coupling between the two fields. This backscattering is characterized by an amplitude  $k$  and a phase  $\phi_k$ . The intrinsic backscattering is, in general, asymmetric due to unavoidable imperfections introduced during device fabrication. Moreover, asymmetries in backscattering are introduced externally in our setup (see Fig. 1), such as reflections at the fiber tip at one side of the chip. An asymmetry  $\delta k$  is therefore introduced in the backscattering amplitude, which in previous work led to the prediction and eventual observance of excitability in SRLs [17]. A similar asymmetry could be added in the backscattering phase, but does not alter the observed dynamics [23] and is therefore not included in Eqs. (1)-(3)

Due to the linear backscattering, SRLs have the tendency to lase in a bidirectional mode. Nevertheless, the two counter-propagating modes saturate both their own and each others gains through spectral hole burning and carrier heating effects. These self- and cross-saturation effects are essential to understand why SRLs can operate in a unidirectional regime. They can be added

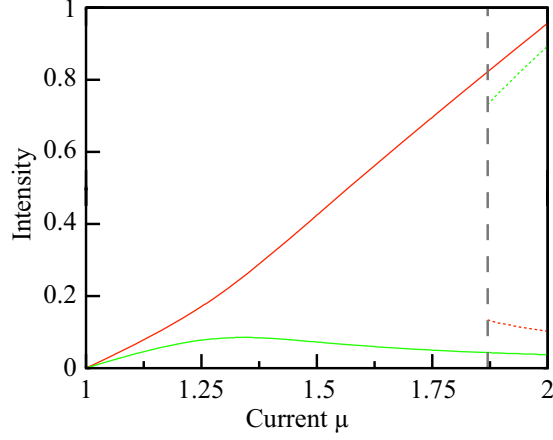


Fig. 5. Mode resolved optical intensity of the CW mode ( $|E_{cw}|^2$ , green) and the CCW mode ( $|E_{ccw}|^2$ , red) vs. injection current  $\mu$  for a solitary SRL ( $\eta = 0$ ) without noise ( $\beta = 0$ ) obtained by numerical integration of Eqs. (1)-(3). Full lines and dashed lines represent different stable attractors.

phenomenologically and are modeled by  $s$  and  $c$ , as:

$$G_{ccw} = 1 - s|E_{ccw}|^2 - c|E_{cw}|^2, \quad (4)$$

$$G_{cw} = 1 - s|E_{cw}|^2 - c|E_{ccw}|^2. \quad (5)$$

Finally, to match the numerical results with experiment, we have included additive Langevin noise terms  $\tilde{F}_{cw,ccw}$  with zero mean and  $\langle \tilde{F}_i(t) \tilde{F}_j^*(t') \rangle = 2\beta \delta_{ij} N \delta(t - t')$  with  $i, j = \{cw, ccw\}$ . We would like to point out that the square wave oscillations are observed in the numerics regardless of the presence of noise.

The remaining parameters in Eqs. (1)-(3) are the linewidth enhancement factor  $\alpha$ , the normalized injection current  $\mu$ , the field decay rate  $\kappa$  and the carrier inversion decay rate  $\gamma$ . In accordance with previous experiments [23], we fix the parameters to the following values:  $s=0.005$ ,  $c=0.01$ ,  $\kappa=100\text{ns}^{-1}$ ,  $\gamma=0.2\text{ns}^{-1}$ ,  $k=0.44\text{ns}^{-1}$ ,  $\phi_k=1.5$ ,  $\alpha=3.5$ ,  $\delta k=0.2$  and  $\beta=5 \cdot 10^{-5}\text{ns}^{-1}$ . In Fig. 5, we show the modal intensity, CCW in red and CW in green, as a function of injected current  $\mu$  for a solitary SRL ( $\eta = 0$ ) without noise ( $\beta = 0$ ). The SRL achieves lasing at  $\mu \approx 1$ . Above and close to the threshold, the SRL resides in the bidirectional regime where it emits in both directional modes with comparable power. The CCW mode increases more strongly than the CW mode with increasing injections current and above  $\mu \approx 1.3$ , the CW mode's power drops and the SRL enters the uni-directional regime where one of the directional modes is much stronger than the other. We also observe a regime of bistability starting at currents higher than  $\mu \approx 1.8$  (beyond the dashed line in Fig. 5). In this regime, emission with high power in the CW mode becomes stable. Comparing Fig. 5 with Fig. 2, we can see that there is a good correspondence between numerics and experimental behavior of the solitary SRL, stressing the validity of the used parameter values.

In what follows, we will turn the delayed cross injection on ( $\eta > 0$ ) and we choose the feedback phase  $\theta = \phi_k$ . We will show later in Section 4 that the feedback phase -contrary to EELs and VCSELs- influences the square wave behavior. Nevertheless, square waves are observed for any feedback phase.

We start by keeping the injection current fixed ( $\mu = 1.65$ ), while analyzing the effect of the feedback strength. Without feedback ( $\eta = 0$ ), we find that due to asymmetric backscattering the



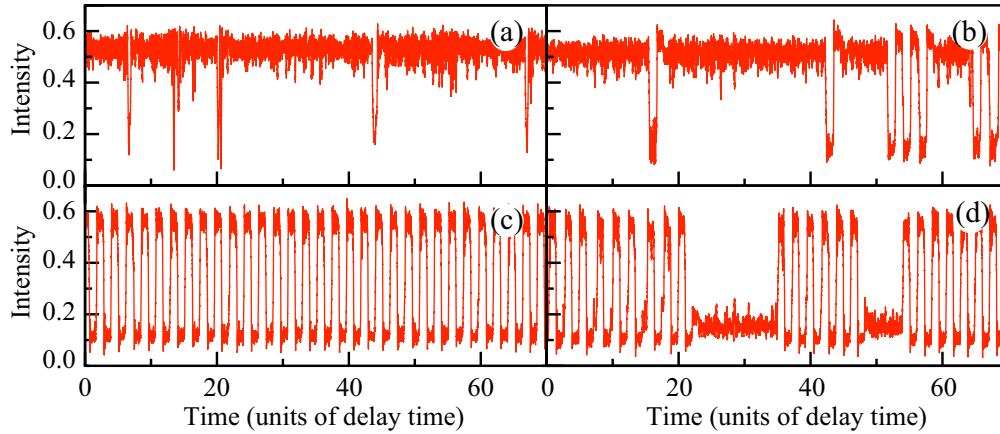


Fig. 6. Intensity of the CCW mode obtained by numerical integration of Eqs. (1)-(3) with  $\mu = 1.65$ , (a)  $\eta = 0.115\text{ns}^{-1}$ , (b)  $\eta = 0.167\text{ns}^{-1}$ , (c)  $\eta = 0.22\text{ns}^{-1}$ , and (d)  $\eta = 0.273\text{ns}^{-1}$ .

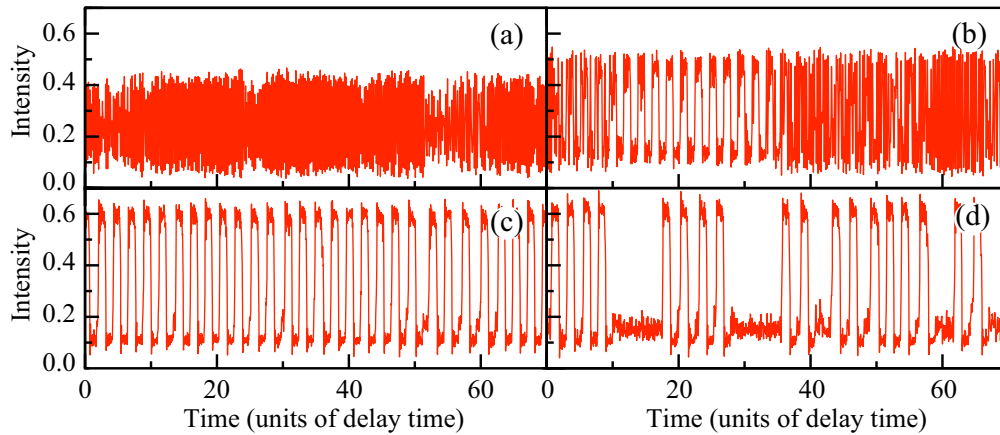


Fig. 7. Intensity of the CCW mode obtained by numerical integration of Eqs. (1)-(3) with  $\eta = 0.22\text{ns}^{-1}$ , (a)  $\mu = 1.5$  (b)  $\mu = 1.58$ , (c)  $\mu = 1.68$ , and (d)  $\mu = 1.7$ .

SRL is mostly lasing in the CCW mode with occasional noise activated excitable excursions to the CW mode [17]. Square wave oscillations are readily obtained when the feedback strength overcomes the asymmetry in the device, i.e.  $\eta = 2k\delta k \approx 0.18\text{ns}^{-1}$ . In Fig. 6, we plot the intensity of the CCW mode,  $|E_{ccw}|^2$ , for different amounts of feedback strength. When  $\eta$  is too weak, the observed behavior is reminiscent of the solitary excitable SRL [see Fig. 6(a)] with short excursions to the CW mode (corresponding to a low power in the CCW mode). However, increasing  $\eta$ , we first observe in Fig. 6(b) noise excited excursions which resemble square wave oscillations. Then, we find fully developed square waves for a range of  $\eta$  values [see Fig. 6(c)], with a period of 110ns. When the feedback strength is increased further in Fig. 6(d), the square wave oscillations degrade exhibiting stochastic hopping to a steady lasing CW mode. From a certain feedback strength on, square wave oscillations no longer appear. We stress here, that the regime of fully developed square wave oscillations (around  $\eta \approx 0.18\text{ns}^{-1}$ ) is also obtained in the absence of spontaneous emission noise ( $\beta = 0$ ) in the numerics. Square waves are then observed in a slightly narrower parameter region, but are nevertheless stable.

In Fig. 7, we investigate the effect of the injection current  $\mu$  on the square wave behavior

while the feedback strength is unaltered ( $\eta = 0.22\text{ns}^{-1}$ ). At low injection current, in Fig. 7(a), we observe alternate oscillations which is a typical dynamical regime of a solitary SRL. The CCW and CW mode oscillate in anti-phase at a frequency of about 100MHz. When the current is increased, we find numerically a stochastic hopping between the aforementioned alternate oscillation limit cycle and the square wave oscillations which have a clearly longer period [see Fig. 7(b)] of approximately 110ns. Then follows an extended current regime where the square waves are fully developed as in Fig. 7(c). Eventually, when  $\mu$  is increased further, we observe first a hopping between square wave oscillations and a steady lasing CW mode [in Fig. 7(d)], and then a disappearance of the square waves in favor of the CW mode.

#### 4. Discussion

Comparing the results from Sec. 2 and Sec. 3, we find a good agreement between experiments and numerical simulation. The numerics show that the square waves are only obtained when both backscattering (linear coupling) and gain saturation (nonlinear coupling) are present in the model. Also, an asymmetry in backscattering is essential to obtain square wave behavior in a certain parameter regime: when setting  $\delta k = 0$  no square waves can be observed. This leads us to conclude that the underlying mechanism for square wave oscillations is the interaction between asymmetric backscattering (i.e. asymmetric linear coupling between the two counter-propagating modes) and the delayed injection of one propagating mode into the other. Without cross-injection, the asymmetry is such that it favors a higher intensity in the CCW mode than in the CW mode. With delayed cross-injection, the low intensity CW mode will receive delayed feedback from the high intensity CCW mode. Effectively, the CW mode then perceives a higher backscattering contribution to its field. As a result the energy between the modes will be repartitioned such that the CW mode now has the higher intensity, while the CCW mode a lower one. After one delay time, the power of the cross injection therefore drops and the SRL returns to the original mode partitioning, leading to the square wave pattern. Because the main mechanism is not relying on gain anisotropies, the two modes involved do not simply switch on and off. Rather, the square wave phenomenon here is a periodic modal energy repartitioning. Square waves then appear in a parameter region roughly in the vicinity of  $\eta = 2k\delta k$ , or when the cross-injection overcomes the built-in asymmetry. If the feedback strength is too weak, the cross-injection might simply bring the SRL in a bistable situation, where it will depend on noise triggers if a square wave cycle will be excited or not. If the feedback strength is too strong, it will effectively reverse the effect of the anisotropy and stabilize a mode partitioning with higher intensity in the CW mode than in the CCW mode. There will be a lower limit on the injection current needed to observe square waves, because at low currents the difference in output power of the two directional modes is too small. For higher injection currents, the higher output power and the gain saturation processes lead to bistable unidirectional operation, hindering the formation of square waves.

The square waves have a duty cycle of about 50% and a period slightly larger than twice the delay time (here: 110 ns). For higher injection currents and/or feedback strengths we see in the simulations of Figs. 6(d) and 7(d) that the square waves disappear through a region in which we can observe bursts of square waves. These apparent bursts of square waves originate from stochastic hopping between a steady-state attractor of one of the uni-directional modes and the square waves behavior. The irregularities observed in the time traces of Fig. 3(c) and Figs. 4(c) and 4(d) can be interpreted as such stochastic hoppings. In order to further experimentally support these numerical observations, we plot in Fig. 8 additional time traces that were recorded for a slightly different fiber alignment as compared to Section 2. In Fig. 8(a) regular square waves are present. By increasing the SRL injection current as shown in Figs. 8(b) and 8(c), we eventually reach the regime as predicted by the simulations in Fig. 6(d) where we observe bursts

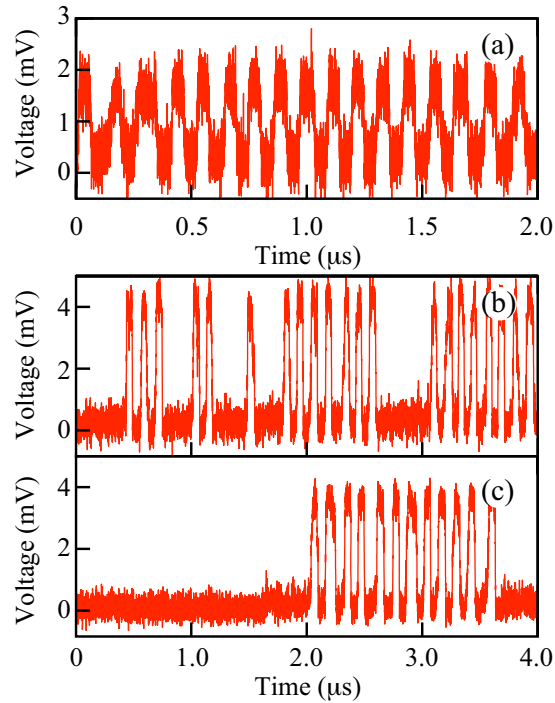


Fig. 8. Time traces of the CCW mode. Parameters are (a)  $I_r = 42\text{mA}$ ,  $I_{SOA} = 300\text{mA}$  and  $I_{WG} = 10\text{mA}$ , (b)  $I_r = 43\text{mA}$ ,  $I_{SOA} = 300\text{mA}$  and  $I_{WG} = 9\text{mA}$  and (c)  $I_r = 44\text{mA}$ ,  $I_{SOA} = 300\text{mA}$  and  $I_{WG} = 14\text{mA}$ . Remark that the intensity levels in the subfigures are slightly different from each other because of the different waveguide currents.

of square waves due to hopping. Comparing Figs. 8(b) and 8(c) we can see that the residence time of the uni-directional emission in this hopping region increases with increasing injection currents, which is also in agreement with numerics.

In Ref. [9], the regular square wave switching dynamics was interpreted in terms of a two-mode rate-equation model, which -however- showed that the square wave behavior is a transient dynamics, sustainable by noise in experimental conditions. It has been shown in Ref. [10] that by including self- and cross- gain saturation and a frequency detuning between the two (polarization) modes in the modeling, stable square waves can be found in certain small parameter regions. The transient dynamics of square wave switchings was also studied recently for two-coupled VCSELs [24]. In the case of SRLs, we have investigated the transient properties of the switching dynamics by analyzing Eqs. (1)-(3) without noise ( $\beta = 0$ ). In Fig. 9, we show a typical time trace of the intensity of the two counter-propagating modes and of the total intensity. The period of the oscillations in our setup is 110ns, which is slightly larger than twice the delay time ( $\tau = 50\text{ns}$ ). Numerically, the square waves are obtained from random initial conditions and once reached remain stable. The origin of the stabilization is yet unknown. One possibility is the presence of the nonlinear gain processes in the model as in [10]. However, this cannot be validated as without gain saturation square waves are not obtained (even with noise). A second possible stabilization mechanism is related to the slow time scale dynamics in SRLs which is due to the underlying  $Z_2$  symmetry of the device [16]. This slow time dynamics is apparent in Fig. 9. The oscillations which accompany the switch from one mode to the other have a frequency of about 120 MHz, a frequency which is associated to the alternate oscillations [which

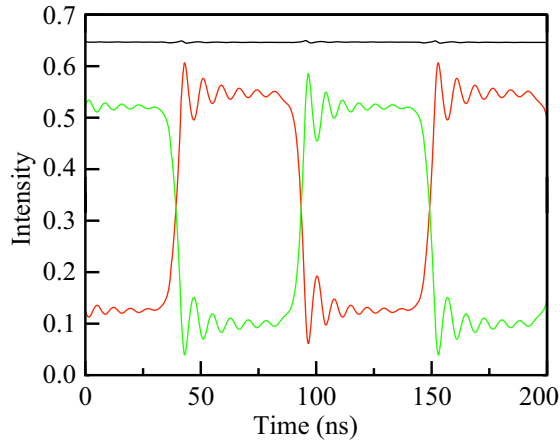


Fig. 9. Mode resolved intensity of the CCW mode (red) and CW mode (green) and total intensity (black) obtained by numerical integration of Eqs. (1)-(3) with  $\eta = 0.19\text{ns}^{-1}$ ,  $\mu = 1.65$  and  $\beta=0$ .

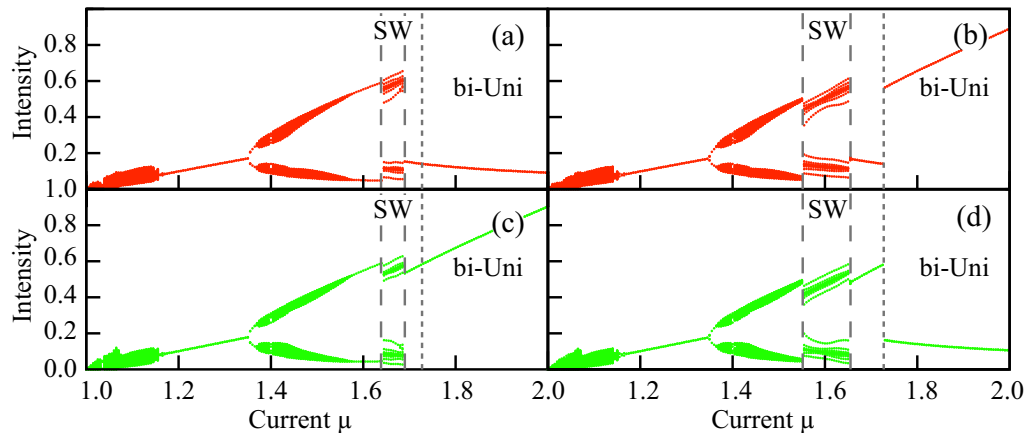


Fig. 10. Orbit diagrams of mode resolved intensity of the CCW mode (red) and CW mode (green) vs. injection current  $\mu$  obtained by numerical integration of Eqs. (1)-(3) with  $\eta = 0.22\text{ns}^{-1}$ ,  $\theta = 1.5$  and  $\beta = 0$ . In (a) and (c),  $\mu$  is ramped up, while in (b) and (d), it is scanned downwards. SW: square waves. bi-Uni: bistable unidirectional regime.

were also shown in Fig. 7(a)]. The total intensity remains constant throughout the square wave oscillations (showing only very minute deviations at a faster time scale related to the relaxation oscillations) and, as such, the modal intensities of CW and CCW are highly anti-correlated. Similarly, the carriers evolve hardly (not shown) and remain very close to the corresponding steady state level. If the total power is conserved and when there is hardly any carrier dynamics, we have motivated in [15,20] that the dynamical behavior of a solitary SRL is confined within a slow (2D) center manifold and organized by a Takens-Bogdanov point with symmetry or with weakly broken symmetry as in [17]. Therefore, the observation of a constant total intensity, carrier level and alternate oscillations within the square wave oscillations, indicates that it is this slow time dynamics that is involved in the formation of the square wave switchings.

In order to probe the onset and degradation of the square wave behavior, we will analyze

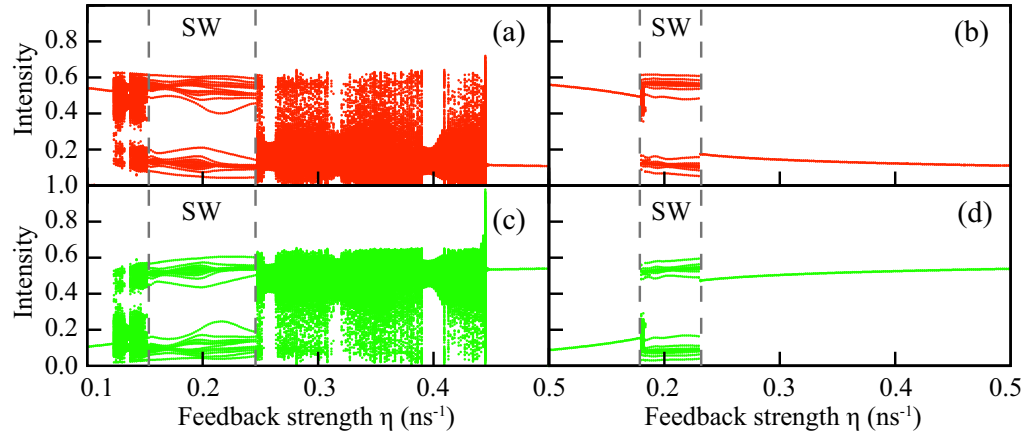


Fig. 11. Orbit diagrams of mode resolved intensity of the CCW mode (red) and CW mode (green) vs. feedback strength  $\eta$  obtained by numerical integration of Eqs. (1)-(3) with  $\mu = 1.65$ ,  $\theta = 1.5$  and  $\beta = 0$ . In (a) and (c),  $\eta$  is ramped up, while in (b) and (d), it is scanned downwards. SW: square waves.

orbit diagrams (sometimes also referred to as bifurcation diagrams). While scanning specific parameters, we follow stable attractors obtained by numerical simulation of Eqs. (1)-(3) without noise ( $\beta = 0$ ). We will plot the extremes of the modal intensities of the CW and CCW modes. In Fig. 10(a) and (c), we plot orbit diagrams of the mode resolved intensities of the CCW mode (red) and the CW mode (green) when increasing the injection current. The delayed cross feedback induces complex dynamics near threshold and when the current is increased, stabilizes a bi-directional emission regime with near equal power in both modes at  $\mu \approx 1.2$ . Above  $\mu \approx 1.3$  alternate oscillations occur. For a small current region, this cycle develops quasi-periodic behavior, but it eventually returns to its periodic state. Then square waves appear at  $\mu \approx 1.6$  and disappear for slightly higher current at which the emission stabilizes with high power in the CW mode. When performing the same analysis by ramping the current down [see Fig. 10(b) and (d)], the square waves are observed in a much wider current range indicated by SW. This indicates multistability between the square wave attractor, alternate oscillations and a stable CW emission. It's clear that above a current of  $\mu \approx 1.7$ , the SRL is bistable indicated by bi-Uni.

In Fig. 11, we again study orbit diagrams but now for varying feedback strength  $\eta$ . It is clear that the square waves phenomenon has a lower and upper limit in feedback strength. The orbit diagrams of Figs. 11(a) and 11(c) show that the onset and degradation of the square waves is accompanied by chaotic dynamics. However, if we add noise to the numerical simulations this chaotic behavior is not observed. As observed in [25, 26], it is common that chaotic attractors in delayed feedback systems are influenced by noise and can even lose their stability. By comparing Fig. 11(a) and 11(b), we can see that at low feedback strengths, the square waves co-exist with stable emission with high power in the CCW mode. At higher feedback strengths, the square waves co-exist with stable emission with high power in the CW mode.

In Fig. 12, we study the effect of the feedback phase on the stability of the square waves dynamics. We would like to note that in EELs and VCSELs, the phase of the cross injection does not play a role. However, in SRLs an effect of the feedback phase cannot be excluded as the two counter-propagating modes are always phase locked through backscattering. Nevertheless, from Fig. 12, it is clear that the square wave forms persist for any feedback phase  $\theta$ . Even more, the stable square wave attractor extends over several times  $2\pi$ . If one would reduce this entire solution to within an interval of length  $2\pi$ , it is clear that the square wave behavior itself

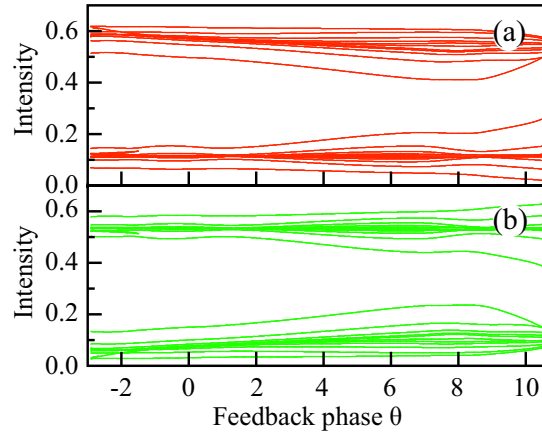


Fig. 12. Orbit diagrams of mode resolved intensity of the CCW mode (red) and CW mode (green) vs. feedback phase  $\theta$  obtained by numerical integration of Eqs. (1)-(3) with  $\mu = 1.65$ ,  $\eta = 0.22\text{ns}^{-1}$  and  $\beta = 0$ .

is multistable, with different families of square waves co-existing at the same feedback phase.

In summary, we have shown that stable square-wave oscillations can be invoked in SRLs using delayed optical cross-feedback. Numerical modeling based on rate equations nicely reproduces the experimental findings. Moreover, from the theoretical analysis, we can conclude that an asymmetry in the backscattering is needed. Square waves then appear in a parameter region where the cross-feedback overcompensates the internal asymmetry. Square waves then correspond to a periodic slow repartitioning of modal energies. The unique features of the square wave regime and how it depends on injection current, feedback (or cross-injection) strength and feedback phase have been further scrutinized by bifurcation analysis. This reveals that multistable square wave forms can exist and that the square waves typically appear and disappear through a mode-hopping region, in which the square wave solution exists together with other steady states.

### Acknowledgments

This work was supported by the Belgian Science Policy Office under the project "Photonics@be" and by the European project PHOCUS (EU FET-Open grant: 240763). We acknowledge the Research Foundation-Flanders (FWO) for individual support and project funding. Furthermore, we thank Gabor Mezosi and Marc Sorel for the fabrication of the semiconductor ring lasers on which the experiments have been performed. The technical team of the James Watt Nanofabrication Centre is also gratefully acknowledged for the support in fabricating the devices. We acknowledge Stefano Beri and Thomas Erneux for valuable and insightful discussions.